Netherlands
organization for
applied scientific
research

TNO-rapport

TNO Division of Technology
for Society

P.O. Box 217
2600 AB Delft
Schoemakerstraat 97
2628 VK Delft, The Netherlands

Telex 38071 zptno nl
Fax +31 15 61 68 12
Phone +31 15 69 69 00

Publication no.: P 88/040

Authors: R.D. Crommelin
E. Buringh

VALIDATION OF A MULTIPLE CELL MODEL FOR THE PREDICTION OF AIR TEMPERATURES AND POLLUTION CONCENTRATIONS BY MEASUREMENTS IN AN INDUSTRIAL HALL

Date: 1988-07-22

Order no.: 17777

Department of Indoor Environment

VALIDATION OF A MULTIPLE CELL MODEL FOR THE PREDICTION OF AIR TEMPERATURES AND POLLUTION CONCENTRATIONS BY MEASUREMENTS IN AN INDUSTRIAL HALL

R.D. CROMMELIN and E. BURINGH

TNO Division of Technology for Society, Department of Indoor Envrionment, P.O. Box 217, 2600 AE Delft, the Netherlands

ABSTRACT

A multiple cell model has been developed for an industrial hall to calculate temperatures and concentrations of air pollution. In this hall air velocities, temperatures and concentrations have been measured. Also smoke tests have been made to study the air flow pattern.

The temperatures and concentrations were calculated for steady state conditions and for a sudden start of the production of heat and pollution when temperatures and concentrations build up from zero to constant values. The calculated steady state concentrations and temperatures are compared with the measured values. A good measure for the accuracy of the prediction by calculations with the model is the standard deviation of the differences between measured and calculated values. For the temperatures the standard deviation is about 1 K and for the concentrations this is about 0.16 mg.m^{-3}, i.e. about 30% of the average concentration. The local deviations are highest at places with strong gradients, i.e. near sources and in convective flows.

The model provides a good method for predicting the dispersion of heat and air pollution in large or smaller enclosures (industrial halls or rooms). The dynamic version of the model can be used for control strategies in air pollution or temperatures.

1. INTRODUCTION

Dispersion of heat and air pollution can be unpleasant or even hazardous, especially in large enclosures like industrial halls. In order to get acceptable working conditions it is desirable to predict temperatures and concentrations of air pollutants in advance. In that case proposed measures for improvements can be studied before they are realized.

Prediction of temperatures and concentrations is possible by:

- mathematical models;
- scale models

To study the air movements in industrial halls under influence of the wind and heat sources and the dispersion of heat and air pollutants caused by these air movements measurements were taken in an industrial hall [1]. In a later study a scale model of this hall was built and temperatures and concentrations (tracer gas) were measured in this model [2]. The measurements in the model were compared with the measurements in the hall itself taking into account the laws for scale models. A mathematical model which calculates the air flows in an enclosure requires the numerical solution of the Navier-Stokes equations in a large number of grid points. This means a large computational effort. In this study a more simplified approach has been followed. The hall was divided into a number of cells and the air flow between the cells are estimated from the measurements in the hall. The supply of air from outside and the exhaust air are simulated by external air flows to and from the relevant cells. With these air flows and the specified sources of heat and air pollution the temperatures and pollution concentrations could be calculated by a multiple cell model. This model only calculates convective transports of heat and pollution. In case of heat transport there is also heat loss by transmission through the roof. This can be simulated in the model by heat sink in the cells under the roof. There is no heat loss through the side walls because the hall is enclosed by other halls with about equal temperatures.

With a multiple cell model different cases of transport of heat and pollution can be studied with much less effort than is possible with scale models or measurements in the hall itself. However, the air flows must be completely specified before whereas a scale model provides information about the flow field.

2. THE MULTIPLE CELL MODEL

The air flows and convective transport processes in the hall are approximated as 2-dimensional. The hall is divided into a number of rectangular cells. For each cell (see Fig. 1) the mass balance for the air flows gives

$$A_{kl}^{ij}\,\rho^{kl} + S^{ij}\,\rho^{e} - A_{ij}^{ij}\,\rho^{ij} = 0 \qquad (1)$$

In this equation A_{kl}^{ij} is the volume flow of cell kl to cell i j, S_{ij}^{ij} is the air flow supplied from outside, A^{ij} is the total air flow from the cell and ρ is the air density. In Equation (1) according to the tensor notation summation over the neighbour cells kl is applied. In the hall the changes in density are small and therefore the density is considered as constant.

Equation (1) reduces to a balance of volume flows:

$$A^{ij}_{kl} + S^{ij} - A^{ij}_{ij} = 0 \qquad (2)$$

$(k,l \neq i, j)$

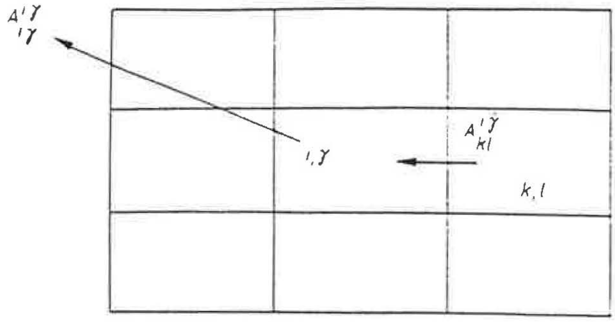

Fig. 1. Air flow from cell k, l to cell i, j.

The heat balance for a cell i, j gives:

$$V\frac{dT^{ij}}{dt} = A^{ij}_{kl}T^{kl} + P^{ij} + S^{ij}T^{o} - A^{ij}_{ij}T^{ij} \qquad (3)$$

In this equation V is the cell volume, that is the product of the cell surface in Fig. 1 and the hall width. P^{ij} is the heat production in cell i, j divided by the product of the density and specific heat (ρc) of air. T^{o} is the average temperature of the air outside the hall.

Equation (3) can also be used for the mass balance of air pollution if T^{ij} is replaced by the concentration C^{ij}. The term P^{ij} is then the production of pollution in cell i, j. The concentration in the supply air is assumed to be 0 in the calculations so the third term in Equation (3) becomes 0. In that case the balance for the air pollution is:

$$V\frac{dC^{ij}}{dt} = A^{ij}_{kl}C^{kl} + P^{ij} - A^{ij}_{ij}C^{ij} \qquad (4)$$

Figure 2 gives a lengthwise section of the hall with the cells. The arrangement of the cells agrees with the places in the hall where measurements have been taken.

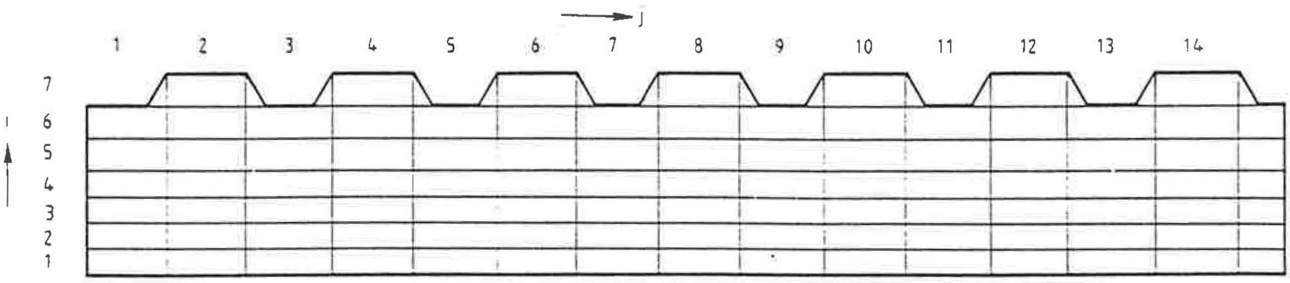

Fig. 2. Lengthwise section of the hall with the arrangement of the cells.

As can be seen from Fig. 2 the index i varies from 1 to 7 and j varies from 1 to 14. Because of the varying height of the roof only half of the top row cells (i = 7) belong to the enclosure of the hall.

In steady state condition the left hand side of Equations (3) and (4) becomes 0. The equations can then be written as:

$$A^{ij}_{kl}T^{kl} + P^{ij} = 0 \qquad (5)$$

$$A^{ij}_{kl}C^{kl} + P^{ij} = 0 \qquad (6)$$

A^{ij}_{ij} is included in A^{ij}_{kl} (k = i and l = j). In Equation (5) T is the increase of the inside air temperature above the average outside air temperature. Equations (5) and (6) are systems of linear equations which can be solved with well-known solution techniques. In our case we have 98 equations with 98 unknowns. The solution techniques can handle only 1-dimensional and 2-dimensional matrices, however, and therefore Equations (5) and (6) must be written as follows:

$$A^{i}_{j}T^{j} + P^{i} = 0 \qquad (7)$$

$$A^{i}_{j}C^{j} + P^{i} = 0 \qquad (8)$$

This implies transformation of 4-dimensional tensors to 2-dimensional tensors and transformation of 2-dimensional tensors to vectors. The indices i and j in Equations (5) and (6) are combined to one index varying from 1 to 98. Two solution techniques have been used, namely the matrix inversion method and the conjugate gradients square (CGS) method. With matrix inversion the inverted matrix B of the matrix A is determined ($B = A^{-1}$). The temperatures and concentrations are calculated by the following equations:

$$B^i_j P^j + T^i = 0 \tag{9}$$

$$B^i_j P^j + C^i = 0 \tag{10}$$

For the matrix inversion a standard routine provided by the computer firm in machine language could be used. This has the advantage that the user does not need to write algorithms to solve the equations but only needs to provide input data (air flows, production rates, air supply).

The computer time for the calculation is about 5 minutes in our case where the matrix A has 98x98 elements. This computer time is strongly dependent on the number of elements, however. Moreover it requires large storage capacity for the matrices A and B where only about 500 of the ca. 10,000 elements are different from 0. Matrix inversion therefore is a very easy but also a very inefficient method. In a more detailed simulation where the enclosure was divided in 4x98 instead of 98 cells matrix inversion was impossible with the available computer facilities.

A more efficient method to solve large systems of linear equations is the Conjugate Gradients Squared method as developed by the Technical University of Delft. For a description of the method the reader is referred to the report [3]. By using this method the computing time required to solve the equations for 98 cells was about 2 minutes instead of 5 minutes required when applying matrix inversion. For the 4x98 cells the computing time was about 12 minutes.

As non-stationary condition the built-up of overtemperatures and concentrations from 0 to the steady state calculated by Equations (7) and (8) has been considered. The initial concentrations and overtemperatures are zero and at each moment the concentration and overtemperature are calculated from their value at a previous moment by the following equations:

$$T^i_{t+1} = T^i_t + (A^i_j\ T^j + P^i)\,dt/V \tag{11}$$

$$C^i_{t+1} = C^i_t + (A^i_j\ C^j + P^i)\,dt/V \tag{12}$$

(dt = timestep between two moments)

As the production terms P are supposed to be constant the overtemperatures and concentrations approach to a constant value after a sufficient long time. But if the production terms or air flow terms are specified as functions of time the overtemperature and concentration in each cell at each moment under these varying circumstances can be calculated with Equations (11) and (12) just as well.

3. THE FACTORY HALL

The hall in question is entirely enclosed by other work halls. The ground plan of the hall is rectangular and there are openings in the walls connecting it with the adjacent halls (see Fig. 3). In the north and south walls are windows which can be opened. The roof has seven high parts and eight low parts. In each of the five high parts counted from the west side of the roof an exhaust fan has been installed. In the hall are two electrotinning machines (ET1 and ET2). Each machine is locally exhausted. The most important heat sources are the two fusion ovens in which the tinplate surface is heated up to the melting point of tin. The most important air pollutant is the oil mist escaping from the tinning plant lubricating system.

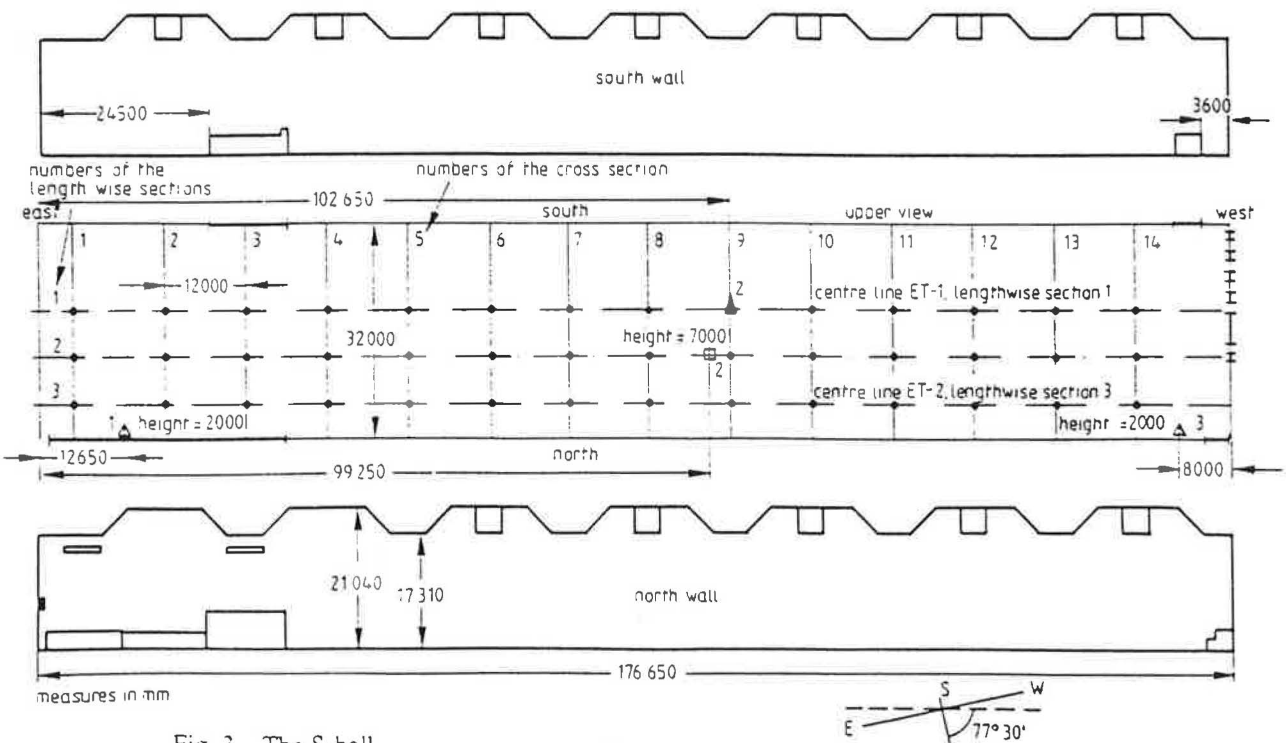

Fig. 3. The S-hall.

From Fig. 3, it can be seen that the hall was divided geometrically into 14 cross sections and three longitudinal planes. Two of the latter planes pass through the center lines of the machine, and the remaining plane passes between the machines. Concentrations, temperatures and air velocities were measured in the intersection points of the planes at distances of 2.75 m above each other. These measurements were made from a crane which could move in lengthwise direction through the hall above the machines. The crane was also used for smoke tests to determine the flow direction in each measuring point.
Figure 4 shows the results of the smoke tests and Fig. 5 the temperatures measured under the low parts of the roof. It was impossible to take the measurements in all 14 cross sections in one day. Longer measuring periods were unacceptable because the weather conditions (wind) and plant production could have changed too much. Figure 6 shows the concentrations measured in the hall.

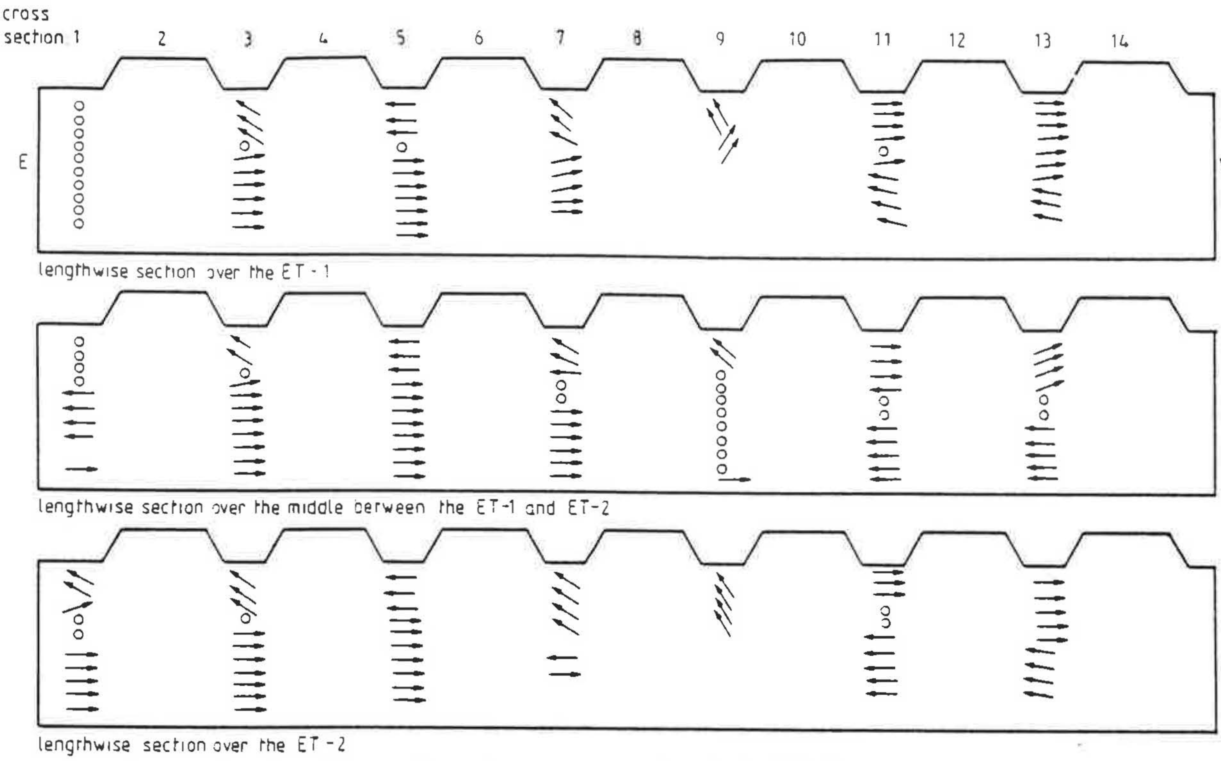

Fig. 4. Direction of the smoke at the measuring points in the S-hall.
→ direction of the smoke
o the smoke travels north

Lengthwise section over the ET-1

cross section: 1	3	5	7	9	11	13
23.9	25.0	26.5	27.6	33.0	28.5	26.7
23.3	24.7	26.5	26.9	33.6	27.0	25.9
23.2	22.8	25.4	25.4	30.6	25.9	24.8
22.9	22.0	24.1	23.8		24.9	24.1
22.7	21.8	22.9	23.7		24.5	23.2
22.3	20.8	22.3			24.1	

lengthwise section over the ET-1

cross section: 1	3	5	7	9	11	13
23.5	24.5	26.5	26.7	30.7	28.6	26.4
23.5	24.2	26.5	26.7	26.8	27.5	26.8
23.4	22.9	24.9	25.4	25.4	25.9	25.1
22.8	22.2	23.8	24.5	25.0	24.6	24.0
22.7	21.8	22.8	23.8	24.8	24.0	23.3
21.9	21.2	21.7	22.6	24.8	23.8	22.4

lengthwise section over the middle between the ET-1 and ET-2

cross section: 1	3	5	7	9	11	13
23.6	25.0	26.3	27.7	33.8	28.5	26.4
23.5	24.9	26.3	27.3	34.2	27.8	26.2
23.3	22.8	24.1	25.4	27.8	25.3	25.1
23.0	22.3	23.2	24.7		24.7	24.0
22.7	22.0	22.6	23.9		24.7	23.8
21.9	21.0	22.2				

lengthwise section over the ET-2

Fig. 5. Temperatures in the S-hall in °C.

cross section: 1	2	3	4	5	6	7	8	9	10	11	12	13	14
	0.7		0.7		1.3		0.8		0.6		0.7		0.5
0.6	0.7	1.0	0.7	1.0	0.9	1.1	0.9	0.7	0.6	0.8	0.7	0.6	0.5
0.6	0.6	0.7	0.8	0.8	0.8	0.8	0.7	0.7	0.4	0.7	0.6	0.7	0.5
0.6	0.6	0.7	0.8	0.7	0.7	0.7	1.0	0.8	0.7	0.6	0.7	0.7	0.5
0.6	0.6	0.7	0.9	0.7	0.7	0.8	0.7			0.6	0.7	0.5	0.4
0.6	0.7	0.7	0.9	0.8	0.6	0.6	1.3			0.7	0.6	0.5	0.4
0.6	0.7	0.7	0.8	0.8	0.6	0.7	influence of machines			0.5	0.6	0.5	0.4

lengthwise section over the ET-1

1	2	3	4	5	6	7	8	9	10	11	12	13	14
	0.6		0.9		1.0		0.9		0.7		0.6		0.5
0.6	0.6	0.5	0.8	1.1	0.8	1.1	0.8	0.8	0.5	1.0	0.6	1.0	0.5
0.6	0.6	0.5	0.8	0.8	0.7	0.9	0.8	0.7	0.4	0.8	0.6	0.9	0.5
0.6	0.6	0.6	0.7	0.7	0.6	0.8	0.7	0.7	0.4	0.6	0.6	0.7	0.4
0.6	0.7	0.6	0.7	0.7	0.7	0.7	0.6	0.8	0.4	0.5	0.6	0.5	0.4
0.6	0.7	0.6	0.7	0.6	0.6	0.7	0.5	0.6	0.5	0.5	0.5	0.5	0.4
0.6	0.6	0.5	0.7	0.7	0.6	0.7	0.5	0.6	0.5	0.6	0.4	0.5	0.4

lengthwise section over the middle between the ET-1 and ET-2

1	2	3	4	5	6	7	8	9	10	11	12	13	14
	0.5		1.0		1.0		1.1		0.6		0.6		0.5
0.6	0.6	0.4	0.9	0.9	0.9	1.4	0.8	0.8	0.6	0.8	0.6	1.0	0.5
0.6	0.6	0.4	0.6	1.0	0.8	1.1	0.9	0.8	0.5	0.7	0.5	0.9	0.5
0.6	0.5	0.5	0.7	0.6	0.7	0.8	1.1	0.9	0.4	0.5	0.5	0.6	0.5
0.6	0.5	0.5	0.6	0.7		0.7	0.8			0.5	0.5	0.5	0.5
0.6	0.5	0.6	0.6	0.7		0.6	1.9			0.6	0.5	0.5	0.6
0.6	0.5	0.6	0.6	0.7		0.6	influence of machines			0.6	0.5	0.5	0.5

lengthwise section over the ET-2

Fig. 6. Mass concentrations of oil mist in the hall ($mg.m^{-3}$).

4. CALCULATED TEMPERATURES

In Fig. 7 the volume flows between the cells and the local heat production are given. The volume flows are estimated from the velocity measurements and smoke tests in the hall. The location of the heat production was found from the temperature measurements and the convection flows above the machines. The volume flows are expressed in $m^3.s^{-1}$ and the heat production terms in $m^3.K.s^{-1}$ as the actual heat production (in W) is divided by the product of the density and specific heat of air (in $J.K^{-1}.kg^{-1}$). The total heat production in the hall then is 2 MW. The heat loss by transmission through the roof is simulated by heat sinks in the cells under the roof.
In Fig. 7 also the air flows to the hall through openings and windows and the air flows from the hall to outside are given. Only average flows are given. In the hall air exchange by turbulence between the cells is assumed. A turbulence velocity of 0.098 $m.s^{-1}$ gave the best agreement between measured and calculated values of temperatures and concentrations. The dimensions of the cells are:

length 12 m
height 2.88 m
width 32 m

This gives turbulent volume flows of 37.6 $m^3.s^{-1}$ in vertical direction and 9 $m^3.s^{-1}$ in horizontal direction. These flows are added to the flows given in Fig. 7.

The outdoor air entering through the windows near the roof fell down to the lower part of the hall because of the large temperature difference (15-20 K). This is represented in Fig. 7 as supply air to the lower cells (i = 1 and 2). Equation (9) only calculates overtemperatures, i.e. the temperature rise in each cell by the heat production. The actual temperature is found by addition of the average outside temperature. This varies slightly over the cross section because of the variation in the outdoor temperature during the day. The average outside temperatures are:

$j = 1,2$: $T_{in} = 13.7°C$
$j = 3\text{-}6$: $T_{in} = 14.1°C$
$j = 7,8$: $T_{in} = 14.5°C$
$j = 9$: $T_{in} = 14.6°C$
$j = 10\text{-}12$: $T_{in} = 14.5°C$
$j = 13,14$: $T_{in} = 14.2°C$

In Fig. 8 the measured and calculated temperatures are given. The calculations have been performed under two conditions, namely with 98 cells, 14 in horizontal direction, and with 4x98 cells, 4x14 cells in horizontal direction. In case of 4x98 cells only the CGS method could be used whereas in case of 98 cells also matrix inversion could be used for the calculation.
With Equation (11) the temperature rise in each cell (98 cells) has been calculated at sudden heat input. In Fig. 9 the temperature rise in two points is illustrated, one point in the upward convective flow with fast temperature response, the other point near the floor with a large air supply and also air flow to the neighbour halls (see Fig. 7) with relatively slow temperature response. The temperature rise in the other cells will be in between the temperature rise of these two points.

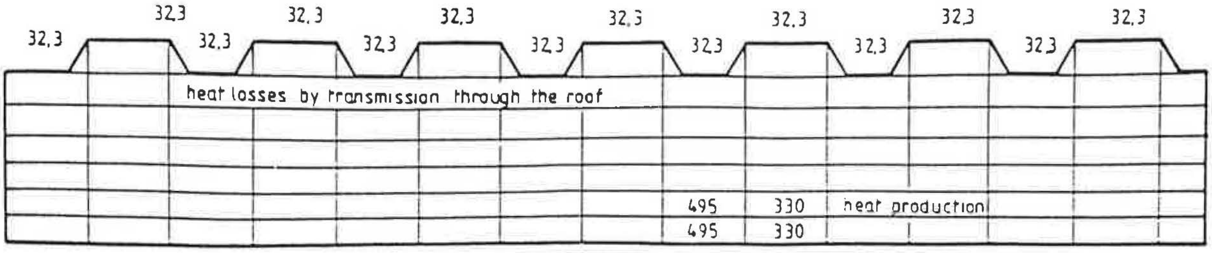

Heat production and losses by transmission ($m^3.K.s^{-1}$)

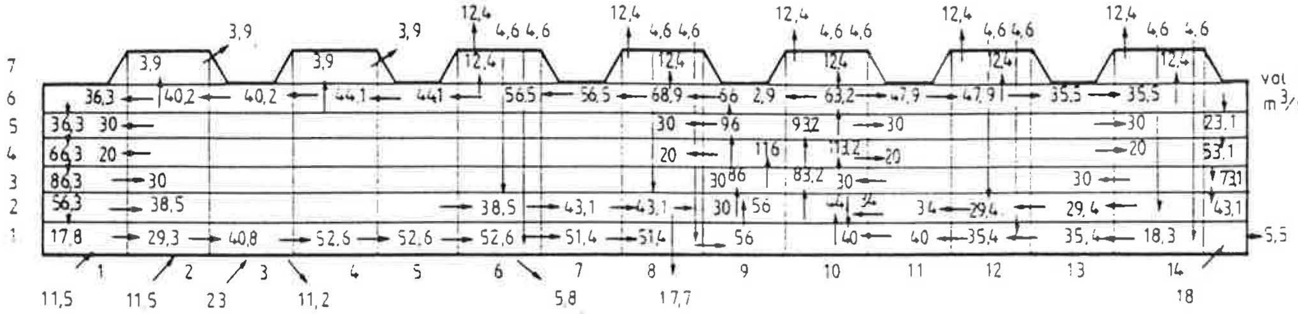

Fig. 7. Volume flows and heat production in the hall (winter condition).

measured temperatures, averaged over 3 lengthwise sections

i \ cross section	1	2	3	4	5	6	7	8	9	10	11	12	13	14
7		-		-		-		-		-		-		-
6	23.7	-	24.8	-	26.4	-	27.3	-	32.5	-	28.5	-	26.5	-
5	23.4	-	24.6	-	26.4	-	27.0	-	31.5	-	27.4	-	26.3	-
4	23.3	-	22.8	-	24.8	-	25.4	-	27.9	-	25.7	-	25.0	-
3	22.9	-	22.2	-	23.7	-	24.3	-	-	-	24.7	-	24.0	-
2	22.7	-	21.9	-	22.8	-	23.8	-	-	-	24.4	-	23.4	-
1	22.0	-	21.0	-	22.1	-	-	-	-	-	-	-	-	-

calculated temperatures, 4x98 cells

i \ cross section	1	2	3	4	5	6	7	8	9	10	11	12	13	14
7		23.0		25.0		25.4		28.5		28.6		25.0		22.0
6	23.3	24.0	25.1	25.8	26.5	27.6	29.5	30.8	32.7	31.4	29.4	27.0	25.0	23.1
5	23.4	24.1	25.0	25.7	26.4	27.5	29.3	30.7	32.8	32.3	29.5	27.2	25.1	23.4
4	23.4	23.7	24.4	24.8	25.4	26.4	27.8	29.0	32.5	32.0	28.3	26.3	24.4	23.2
3	23.3	23.4	23.5	23.8	24.2	24.9	26.1	26.7	.	.	26.5	24.9	23.5	22.8
2	23.1	22.8	22.6	22.8	23.2	23.6	24.6	24.8	.	.	25.0	23.8	22.7	22.3
1	22.8	22.1	21.4	22.0	22.5	22.8	.	.	.	.	.	.	.	21.6

calculated temperatures, 98 cells

i \ cross section	1	2	3	4	5	6	7	8	9	10	11	12	13	14
7		22.7		24.6		26.7		28.8		28.6		27.3		25.7
6	22.9	23.4	24.5	25.4	26.3	27.4	28.6	29.4	30.0	29.2	28.6	28.0	26.9	26.4
5	23.1	23.5	24.4	25.1	25.9	26.8	28.2	29.3	30.4	29.5	28.7	27.9	26.9	26.5
4	23.0	23.0	23.7	24.1	24.7	25.5	26.9	28.4	30.6	29.6	28.1	27.1	26.2	26.2
3	22.8	22.4	22.6	22.8	23.1	23.6	24.7	26.1	-	-	26.6	25.6	25.2	25.6
2	22.1	21.5	21.4	21.5	21.8	21.9	23.1	24.3	-	-	25.4	24.0	23.8	23.8
1	20.6	20.0	19.5	20.3	20.9	21.0	-	-	-	-	-	-	-	21.2

Fig. 8. Measured and calculated temperatures (°C).

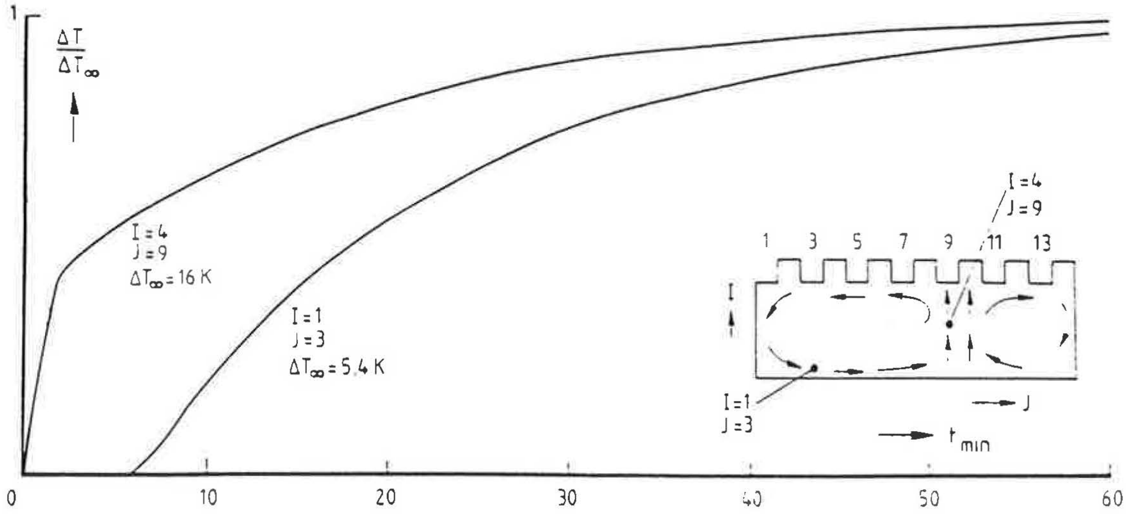

Fig. 9. Temperature rise in two points at sudden heat input.

5. CALCULATED CONCENTRATIONS

The concentrations have been calculated with Equation (10) for steady state conditions and with the same air flows as for the temperatures (see Fig. 7). In this hall the main air pollution is caused by an oil mist which comes from the moving parts of the machines (rotating shafts). In Fig. 10 the cells where pollution is produced are indicated. Fig. 11 shows the measured and calculated concentrations. The concentrations in the convective flow upwards and under the roof are higher than near the floor where fresh air is supplied. With Equation (12) the built-up of the concentration in each cell is calculated if the production of air pollution as indicated in Fig. 11 suddenly starts. Figure 12 shows the concentration rise in the same two points as indicated in Fig. 9 for the temperature rise. The shape of the curves is somewhat different from those in Fig. 9 because the production of air pollution is located at different places as the heat production and not concentrated into a small area. The concentration rise in the other cells is in between the concentration rise in these two cells.

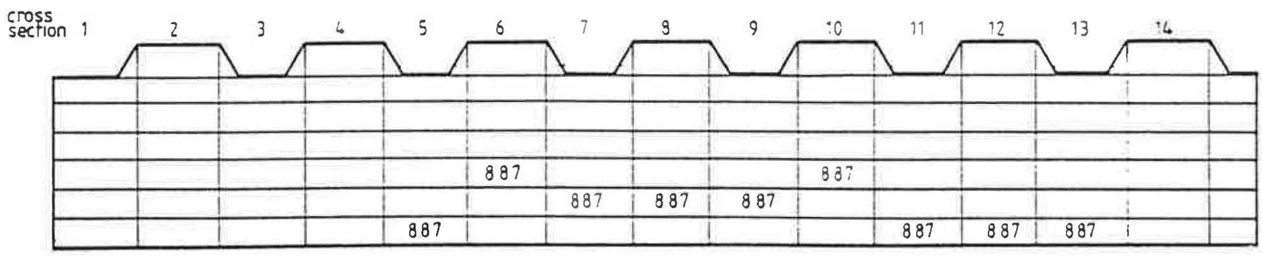

Fig. 10. Production of air pollution (oil mist) in the hall ($mg.s^{-1}$).

i \ cross section (j →)	1	2	3	4	5	6	7	8	9	10	11	12	13	14
7		0.60		0.87		1.10		0.93		0.63		0.63		0.50
6	0.60	0.63	0.63	0.80	1.00	0.87	1.20	0.87	0.77	0.63	0.87	0.63	0.87	0.50
5	0.60	0.60	0.53	0.73	0.87	0.77	0.93	0.80	0.73	0.43	0.77	0.57	0.83	0.50
4	0.60	0.57	0.60	0.73	0.77	0.67	0.77	0.93	0.80	0.50	0.57	0.60	0.67	0.47
3	0.60	0.60	0.60	0.73	0.70	-	0.73	0.70	-	-	0.53	0.60	0.50	0.43
2	0.60	0.63	0.63	0.73	0.70	-	0.63	1.23	-	-	0.60	0.53	0.50	0.47
1	0.60	0.60	0.60	0.70	0.73	-	0.67	-	-	-	0.57	0.50	0.50	0.43

measured concentrations, averaged over 3 lengthwise sections

i \ cross section	1	2	3	4	5	6	7	8	9	10	11	12	13	14
7		0.62		0.69		0.63		0.68		0.64		0.56		0.47
6	0.63	0.64	0.67	0.69	0.69	0.70	0.73	0.75	0.77	0.72	0.69	0.63	0.58	0.53
5	0.63	0.64	0.66	0.68	0.71	0.73	0.74	0.76	0.78	0.77	0.71	0.65	0.59	0.54
4	0.62	0.63	0.63	0.65	0.70	0.76	0.75	0.75	0.78	0.81	0.71	0.64	0.58	0.52
3	0.62	0.61	0.59	0.61	0.66	.	0.74	0.73	.	.	0.71	0.63	0.56	0.50
2	0.62	0.58	0.53	0.57	0.62	.	0.71	0.71	.	.	0.72	0.63	0.55	0.49
1	0.60	0.55	0.47	0.56	0.63	.	0.66	.	.	.	0.78	0.69	0.59	0.47

calculated concentrations, 4x98 cells

i \ cross section	1	2	3	4	5	6	7	8	9	10	11	12	13	14
7		.722		.758		.793		.804		.818		.805		.788
6	.715	.722	.737	.758	.778	.793	.800	.804	.806	.818	.814	.805	.794	.788
5	.707	.704	.714	.734	.760	.785	.794	.801	.805	.819	.809	.795	.783	.780
4	.695	.675	.672	.688	.723	.773	.784	.795	.804	.821	.798	.774	.759	.764
3	.677	.642	.618	.620	.656		.768	.783			.774	.737	.724	.729
2	.627	.580	.537	.545	.600		.752	.783			.778	.706	.680	.626
1	.513	.467	.399	.467	.606		.657				.866	.769	.684	.470

calculated concentrations, 98 cells

Fig. 11. Measured and calculated concentrations ($mg.s^{-1}$).

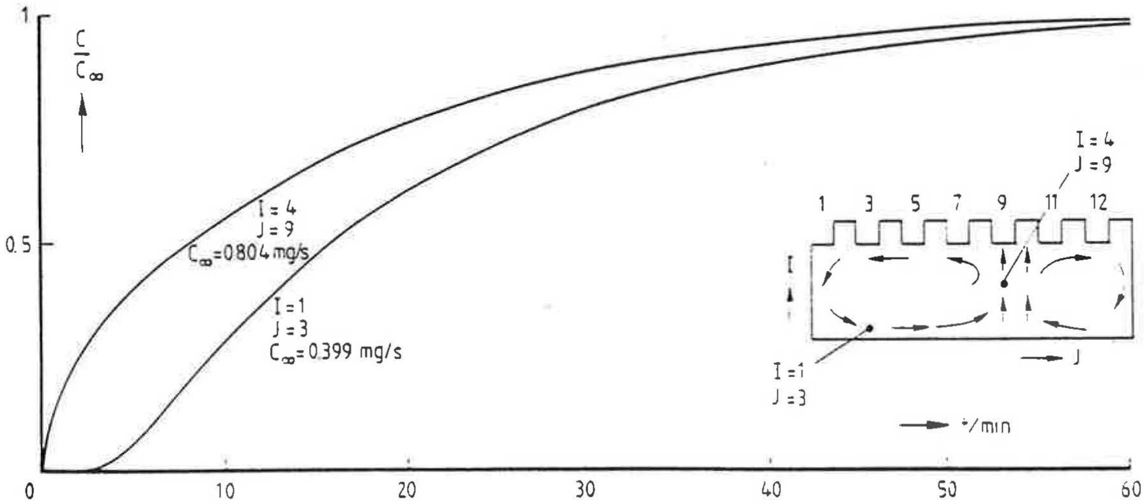

Fig. 12. Concentration rise in two points at sudden production of air pollution.

6. COMPARISON OF CALCULATED VALUES WITH MEASURED VALUES

6.1 Temperatures

In order to compare the calculated temperatures and concentrations with the measured values (see Fig. 8 and 11) the difference between these two values has been calculated for each cell. For each calculation the average value and the standard deviation of these differences were determined. Table 1 gives the results for the temperatures. In this table $T' = \Delta T_{measured} - \Delta T_{calculated}$, $\overline{T'}$ is the average value and $\sigma T'$ is the standard deviation of T'.

Table 1. Comparison between measured and calculated temperatures.

Simulation	$\overline{T'}$ (K)	$\sigma T'$ (K)	$\overline{\Delta T}$ (K)	$\overline{T'}/\overline{\Delta T}$ (%)	$\sigma T'/\overline{\Delta T}$ (%)
calc., 4x98 cells, first period	-0.73	1.16	11.4	6	10
calc., 4x98 cells, second period	-0.43	1.16	11.4	4	10
calc., 98 cells, first period	-0.14	1.14	11.4	1.2	10
calc., 98 cells, second period	1.15	1.02	11.4	10	9
scale model, first period	2.16	2.38	11.4	19	21

The calculations have been compared with temperatures measured in two measuring periods in the winter. In the first period (see Fig. 5) the temperatures were measured under the low parts of the roof, i.e. in the odd numbered cross sections. In the second period temperatures were measured in the cross sections 2-7. Also included in the table is a comparison between measurements in a scale model of the hall (1:20) and the measurements in the hall during the first period [2].
In most calculations the average overtemperature ($\overline{T'}$) deviates less than 1 K from the average overtemperature in the hall and in one calculation this deviation is only slightly more than 1 K. By a slightly modified heat input this average deviation can be made zero. But this will have no influence on the standard deviation of T'. The standard deviation determines the accuracy which can be reached in predicting the temperatures in the hall. In fact it gives the 68% confidence limits. It depends on the fluctuations in the hall temperatures by irregular air movements and possible other causes. These fluctuations are particularly strong near heat sources. The scale model, however, gives higher values of the average value and standard deviation of T'. This indicates that with scale model measurements the accuracy in the prediction of the temperatures is lower in this case than with a mathematical model as described in this paper.

6.2 Concentrations

The oil mist concentrations in the hall have been measured on a summer day and a winter day. On the summer day the air flows entering and leaving the hall (ventilation) was considerably higher than on the winter day because more windows and doors in neighbour hall were open. This caused lower concentrations on the summer day.
As with the overtemperatures the difference between the measured and calculated concentration in each cell was determined. Table 2 gives the average value and standard deviation of these differences. In this table $C' = C_{measured} - C_{calculated}$. The results of the concentration measurements in the scale model simulating the summer day are also included. The average difference between the measured and calculated concentration (C') is very low in most cases. The standard deviation $\sigma C'$ has about the same value in all cases. The scale model measurements do not give a higher value of the standard deviation than the calculations as is the case for the temperatures. Expressed in a percentage of the average concentration the standard deviation is much higher than the standard deviation of T'. This is caused by the different accuracies in the measurements and the different average values of the overtemperatures and the concentrations, respectively.

Table 2. Comparison between measured and calculated concentrations.

Simulation	$\overline{C'}$ (mg.m^{-3})	$\sigma C'$ (mg.m^{-3})	$\overline{C}$ (mg.m^{-3})	$\overline{C'}/\overline{C}$ (%)	$\sigma C'/\overline{C}$ (%)
calc., 4x98 cells, winterperiod	0.018	0.147	0.648	3	23
calc., 4x98 cells, summer period	0.016	0.152	0.480	3	32
calc., 98 cells, winter period	-0.040	0.164	0.648	6	25
calc., 98 cells, summer period	-0.034	0.164	0.480	7	34
scale model, summer period	0.003	0.168	0.480	1	35

7. CONCLUSIONS

Temperatures and concentrations can be predicted with reasonable accuracy by the multiple cell model and by scale models. Temperatures are predicted with greater accuracy by the multiple cell model than by a scale model . Calculations require much less effort than model measurements but require a reliable estimation of the flows between the cells.

8. NOMENCLATURE

A	volume flow tensor ($m^3.s^{-1}$)
B	inverse matrix of A ($s.m^{-3}$)
C	air pollution concentration ($mg.m^{-3}$)
i, j, k, l	indices (see Fig. 2)
P	production of heat ($m^3.K.s^{-1}$) or air pollution ($mg.s^{-1}$)
S	air supply tensor ($m^3.s^{-1}$)
T	temperature (°C)
ΔT	temperature difference (K)
t	time index
dt	time step (s)
V	cell volume (m^3)

REFERENCES

[1] Beukering, F.C. van, P. Boekesteyn and R.D. Crommelin. Die Ausbreitung von Luftverunreinigungen in einer Werkhalle durch Konvektionsströmungen (The dispersion of air pollutants in a work hall by convection currents). *Staub-Reinhaltung der Luft* 33 (1973), no. 4 (April), p. 192-196.

[2] Crommelin, R.D. and P. Maaskant. Modelluntersuchung des Innenklimas in einer Fabrikhalle (A scale model study of the indoor climate in an industrial hall). *Staub-Reinhaltung der Luft* 40 (1980), no. 2 (February), p. 49-58.

[3] Kaasschieter, E.F.. The solution of non-symmetric linear systems by biconjugate gradients or conjugate gradients squared. Delft University of Technology, Department of Mathematics and Informatics, Report No. 86-21, Delft, 1986.